Modeling the efficiency of Förster resonant energy transfer from energy relay dyes in dye-sensitized solar cells

Eric T. Hoke,[1] Brian E. Hardin,[2] and Michael D. McGehee[2]*

[1]*Department of Applied Physics, Stanford University, 476 Lomita Mall, Stanford, CA, USA*
[2]*Department of Material Science and Engineering, Stanford University, 476 Lomita Mall, Stanford, CA, USA*
**mmcgehee@stanford.edu*

Abstract: Förster resonant energy transfer can improve the spectral breadth, absorption and energy conversion efficiency of dye sensitized solar cells. In this design, unattached relay dyes absorb the high energy photons and transfer the excitation to sensitizing dye molecules by Förster resonant energy transfer. We use an analytic theory to calculate the excitation transfer efficiency from the relay dye to the sensitizing dye accounting for dynamic quenching and relay dye diffusion. We present calculations for pores of cylindrical and spherical geometry and examine the effects of the Förster radius, the pore size, sensitizing dye surface concentration, collisional quenching rate, and relay dye lifetime. We find that the excitation transfer efficiency can easily exceed 90% for appropriately chosen dyes and propose two different strategies for selecting dyes to achieve record power conversion efficiencies.

OCIS codes: (260.2160) Energy Transfer; (350.6050) Solar Energy; (160.2540) Fluorescent and luminescent materials; (160.4236) Nanomaterials.

References and links

1. B. O'Regan, and M. Grätzel, "A Low-Cost, High-Efficiency Solar Cell Based on Dye-Sensitized Colloidal TiO_2 Films," Nature **353**(6346), 737–740 (1991).
2. M. K. Nazeeruddin, F. De Angelis, S. Fantacci, A. Selloni, G. Viscardi, P. Liska, S. Ito, B. Takeru, and M. Grätzel, "Combined Experimental and DFT-TDDFT Computational Study of Photoelectrochemical Cell Ruthenium Sensitizers," JACS **127**(48), 16835–16847 (2005).
3. B. E. Hardin, E. T. Hoke, P. B. Armstrong, J. H. Yum, P. Comte, T. Torres, J. M. J. Frechet, M. K. Nazeeruddin, M. Grätzel, and M. D. McGehee, "Increased light harvesting in dye-sensitized solar cells with energy relay dyes," Nat. Photonics **3**(7), 406–411 (2009).
4. P. R. F. Barnes, A. Y. Anderson, S. E. Koops, J. R. Durrant, and B. C. O'Regan, "Electron Injection Efficiency and Diffusion Length in Dye-Sensitized Solar Cells Derived from Incident Photon Conversion Efficiency Measurements," J. Phys. Chem. C **113**(3), 1126–1136 (2009).
5. A. Blumen, J. Klafter, and G. Zumofen, "Influence of restricted geometries on the direct energy transfer," J. Chem. Phys. **84**(3), 1397–1401 (1986).
6. B. K.-K. Fung, and L. Stryer, "Surface density determination in membranes by fluorescence energy transfer," Biochemistry **17**(24), 5241–5248 (1978).
7. J. M. Drake, J. Klafter, and P. Levitz, "Chemical and biological microstructures as probed by dynamic processes," Science **251**(5001), 1574–1579 (1991).
8. G. Calzaferri, and K. Lutkouskaya, "Mimicking the antenna system of green plants," Photochem. Photobiol. Sci. **7**(8), 879–910 (2008).
9. C. Joo, H. Balci, Y. Ishitsuka, C. Buranachai, and T. Ha, "Advances in single-molecule fluorescence methods for molecular biology," Annu. Rev. Biochem. **77**(1), 51–76 (2008).
10. B. Schuler, and W. A. Eaton, "Protein folding studied by single-molecule FRET," Curr. Opin. Struct. Biol. **18**(1), 16–26 (2008).
11. J. P. S. Farinha, and J. M. G. Martinho, "Resonance Energy Transfer in Polymer Nanodomains," J. Phys. Chem. C **112**(29), 10591–10601 (2008).
12. Y. X. Liu, M. A. Summers, C. Edder, J. M. J. Fréchet, and M. D. McGehee, "Using Resonance Energy Transfer to Improve Exciton Harvesting in Organic-Inorganic Hybrid Photovoltaic Cells," Adv. Mater. **17**(24), 2960–2964 (2005).
13. R. Koeppe, O. Bossart, G. Calzaferri, and N. S. Sariciftci, "Advanced photon-harvesting concepts for low-energy gap organic solar cells," Sol. Energy Mater. Sol. Cells **91**(11), 986–995 (2007).

#121278 - $15.00 USD Received 16 Dec 2009; revised 3 Feb 2010; accepted 6 Feb 2010; published 11 Feb 2010

14. T. Förster, "Zwischenmolekulare Energiewnderung und Fluoreszenz," Ann. Phys. **437**(1-2), 55–75 (1948).
15. I. Z. Steinberg, and E. Katchalski, "Theoretical Analysis of the Role of Diffusion in Chemical Reactions, Fluorescence Quenching, and Nonradiative Energy Transfer," J. Chem. Phys. **48**(6), 2404–2410 (1968).
16. D. D. Thomas, W. F. Carlsen, and L. Stryer, "Fluorescence energy transfer in the rapid-diffusion limit," Proc. Natl. Acad. Sci. U.S.A. **75**(12), 5746–5750 (1978).
17. J. R. Lakowicz, *Principles of Fluorescence Spectroscopy,* 3rd ed. (Springer, 2006).
18. J. Baumann, and M. D. Fayer, "Excitation transfer in disordered two-dimensional and anisotropic three-dimensional systems: Effects of spatial geometry on time-resolved observables," J. Chem. Phys. **85**(7), 4087–4107 (1986).
19. M. Grätzel, "Conversion of sunlight to electric power by nanocrystalline dye-sensitized solar cells," J. Photochem. Photobiol. Chem. **164**(1-3), 3–14 (2004).
20. Y. R. Khan, T. E. Dykstra, and G. D. Scholes, "Exploring the Förster limit in a small FRET pair," Chem. Phys. Lett. **461**(4-6), 305–309 (2008).
21. J. Najbar, and M. Mac, "Mechanisms of fluorescence quenching of aromatic molecules by potassium iodide and potassium bromide in methanol–ethanol solutions," J. Chem. Soc., Faraday Trans. **87**(10), 1523–1529 (1991).
22. T. Förster, "Experimentelle und theoretische Untersuchung des zwischenmolekularen Ubergangs von Elektronenanregungsenergie," Z. Naturforsch. B **4a**, 321 (1949).
23. D. Parker, "Luminescent lanthanide sensors for pH, pO2 and selected anions," Coord. Chem. Rev. **205**(1), 109–130 (2000).
24. S. Ito, T. N. Murakami, P. Comte, P. Liska, C. Grätzel, M. K. Nazeeruddin, and M. Grätzel, "Fabrication of thin film dye sensitized solar cells with solar to electric power conversion efficiency over 10%," Thin Solid Films **516**(14), 4613–4619 (2008).
25. L. M. Peter, "Dye-sensitized nanocrystalline solar cells," Phys. Chem. Chem. Phys. **9**(21), 2630–2642 (2007).
26. N. Sabbatini, M. Guardigli, J.-M. Lehn, and G. Mathis, "Luminescence of lanthanide cryptates: effects of phosphate and iodide anions," J. Alloy. Comp. **180**(1-2), 363–367 (1992).
27. Y. Elkana, J. Feitelson, and E. Katchalski, "Effect of Diffusion on Transfer of Electronic Excitation Energy," J. Chem. Phys. **48**(6), 2399–2404 (1968).
28. J.-C. G. Bünzli, and C. Piguet, "Taking advantage of luminescent lanthanide ions," Chem. Soc. Rev. **34**(12), 1048–1077 (2005).
29. J. H. Yum, B. E. Hardin, S. J. Moon, E. Baranoff, F. Nüesch, M. D. McGehee, M. Grätzel, and M. K. Nazeeruddin, "Panchromatic Response in Solid-State Dye-Sensitized Solar Cells Containing Phosphorescent Energy Relay Dyes," Angew. Chem. Int. Ed. **48**(49), 9277–9280 (2009).
30. I. K. Ding, N. Tétreault, J. Brillet, B. E. Hardin, E. H. Smith, S. Rosenthal, F. Sauvage, M. Grätzel, and M. D. McGehee, "Pore-Filling of Spiro-OMeTAD in Solid-State Dye Sensitized Solar Cells: Quantification, Mechanism, and Consequences for Device Performance," Adv. Funct. Mater. **19**(15), 2431–2436 (2009).

1. Introduction

Dye sensitized solar cells (DSCs) [1] are a promising photovoltaic technology that has achieved power conversion efficiencies of over 11% [2]. These devices can obtain high open circuit voltages of 0.85 V and fill factors of 0.75 but are less efficient than many inorganic solar cells primarily because the currently employed dyes achieving the highest power conversion efficiencies do not effectively absorb photons above ~750 nm in wavelength.

We recently demonstrated that energy relay dyes can enhance both the spectral breadth and absorption of dye sensitized solar cells, improving the power conversion efficiency by over 25% [3]. In this design unattached relay dyes (the energy donor) absorb high energy photons and transfer the excitation to the sensitizing dye (the energy acceptor) by Förster resonant energy transfer (FRET). The sensitizing dye directly absorbs the lower energy photons. This design motivates the development of sensitizing dyes that absorb strongly in the near-infrared, which used in conjunction with relay dyes that absorb over the visible wavelengths may enable power conversion efficiencies of 15% to be achieved. For this architecture to achieve a record power conversion efficiency device, a high excitation transfer efficiency (ETE) from the relay dye to the sensitizing dye of over 90% is likely needed. Conventional DSCs frequently have an external quantum efficiency of over 90% at strongly absorbed wavelengths and an internal quantum efficiency of ~95% [4]. Due to the extra step in harvesting photons absorbed by the relay dye, an ETE of less than 90% would likely result in an insufficient external quantum efficiency over the wavelengths absorbed by the relay dye.

Theoretical calculations for the excitation transfer efficiency and dynamics have been performed and experimentally verified for energy donors and acceptors in a variety of geometries and distributions [5–8]. Differences in the geometric arrangement

#121278 - $15.00 USD Received 16 Dec 2009; revised 3 Feb 2010; accepted 6 Feb 2010; published 11 Feb 2010

of $k_F = \frac{1}{\tau_0}\frac{R_0^6}{\left|\mathbf{r_A} - \mathbf{r_D}\right|^6}$ donors and acceptors can have a significant impact on the excitation transfer efficiency and energy transfer dynamics. Much of the recent work has been motivated by the application of using fluorescence spectroscopic methods to measure nanometer scale distances in biological [9,10] and polymeric [11] systems for structural characterization as well as using FRET to enhance the capabilities of nanostructured optoelectronic devices including solar cells [3,8,12,13].

Förster's energy transfer theory [14] has also been extended to account for the effects of chromophore diffusion [15,16]. Diffusion of the donors and/or the acceptors can significantly increase the excitation transfer efficiency since it enables donor and acceptors that are originally too far apart for energy transfer to appreciably occur to move closer together, into range for FRET. This effect is large for dye molecules with long excited state lifetimes (≥ 1 μs) in low viscosity solvents that can diffuse a distance in the excited state that is far greater than the distance over which FRET is effective. Förster resonant energy transfer in the presence of chromophore diffusion has been typically studied in three different regimes: the stationary limit where diffusion is negligible, the rapid diffusion limit where the diffusion length is much larger than the average donor-acceptor separation distance, and the more complex intermediate regime. Different models are used for calculating the excitation transfer efficiency for each regime.

In this paper we present a comprehensive model to compute the excitation transfer efficiency in a dye sensitized solar cell for all three diffusional regimes from relay dyes distributed throughout the mesoscopic pore volume to sensitizing dye molecules densely and uniformly attached to the pore walls. In our model we consider the competing process of collisional quenching of the relay dye fluorescence which can be significant in DSCs since the iodide/triiodide redox couple is a nearly perfect quencher of many dyes [17]. We define a critical distance, R_c, over which the energy transfer process is efficient in this system and which we propose as the figure of merit in selecting dyes for high excitation transfer efficiencies. In Section 3, we present quantitative calculations of the excitation transfer efficiency for pores with cylindrical or spherical geometries and consider the effects of the Förster radius, average pore size, sensitizing dye surface concentration, collisional quenching rate, and relay dye lifetime on the excitation transfer efficiency. We find that the ETE can easily exceed 90% in two different situations: dye combinations with a relatively large Förster radius in which the donor has a short lifetime to avoid quenching effects or alternatively a dye combination which can have a relatively small Förster radius, provided that the relay dye has a long fluorescence lifetime and is not significantly quenched by the electrolyte to enable chromophore diffusion. On the basis of these calculations, we present design criteria for selecting dyes and device architectures to achieve near unity excitation transfer efficiencies.

2. Background and model description

Förster resonant energy transfer is the mechanism for excitation transfer mediated by the coupling of two resonant dipoles through the electric field. The rate of FRET, k_F, from an energy donor at the position vector $\mathbf{r_D}$ to an acceptor at $\mathbf{r_A}$, as shown in Fig. 1(a), is given by:

$$k_F = \frac{1}{\tau_0}\frac{R_0^6}{\left|\mathbf{r_A} - \mathbf{r_D}\right|^6} \tag{1}$$

Here τ_0 is the lifetime of the energy donor excited state, and R_0 is the Förster radius which is the distance over which excitation transfer is 50% probable. The Förster radius can be computed from the energy donor photoluminescence quantum efficiency, $Q_{D,0}$, and overlap integral of the donor emission spectrum F_D with the acceptor absorption spectrum ε_A [17].

$$R_0^6 = \frac{9000 \cdot \ln(10)\kappa^2 Q_{D,0}}{128\pi^5 n^4 N_A}\int F_D(\lambda)\varepsilon_A(\lambda)\lambda^4 d\lambda \tag{2}$$

#121278 - $15.00 USD Received 16 Dec 2009; revised 3 Feb 2010; accepted 6 Feb 2010; published 11 Feb 2010

The other factors occurring in this equation are Avogadro's number, N_A, the dielectric constant of the medium, n, and a dimensionless orientation factor, κ^2, which is equal to 2/3 if the dipoles are randomly oriented and can rapidly reorient. In this article, we define $Q_{D,0}$ such that it accounts for all static quenching effects but does not account for dynamic quenching by other donor dye molecules or chemical species, which we address separately. If multiple acceptors are available, as shown in Fig. 1(b), the total rate of resonant energy transfer is the sum of the rates to each acceptor, since the acceptors act independently.

$$k_F\left(\mathbf{r_D}\right) = \sum_{\mathbf{A_i}} \frac{1}{\tau_0} \frac{R_0^6}{\left|\mathbf{r_{A_i}} - \mathbf{r_D}\right|^6} \tag{3}$$

It is also possible for energy transfer to occur from one donor to another donor which can be the dominant energy transfer process in some systems [18]. However, for DSCs utilizing relay dyes it is preferable for the energy relay dye to have a moderately large Stokes shift so that the absorption bandwidth between the relay and sensitizing dyes is maximized while allowing for efficient FRET from the relay dye to the sensitizing dye. As a result, the Förster radius between donors is typically small compared to the average separation distance between the donor chromophores in the electrolyte (~4 nm) so we can assume that this process is negligible in our model. We note that if relay dyes are used which do undergo appreciable donor-donor transfer, our model provides a conservative estimate for the excitation transfer efficiency.

Knowledge of the exact positions of all of the donors and acceptors is required to make use of Eq. (3). More general theories have been developed to calculate the rate of energy transfer if statistics describing the distribution of acceptors and donors are known [5]. Since there is statistical uncertainty in the positions of individual donors and acceptors, the dynamics of energy transfer from a given donor cannot in general be described by a single rate and must be characterized by a probabilistic distribution of rates.

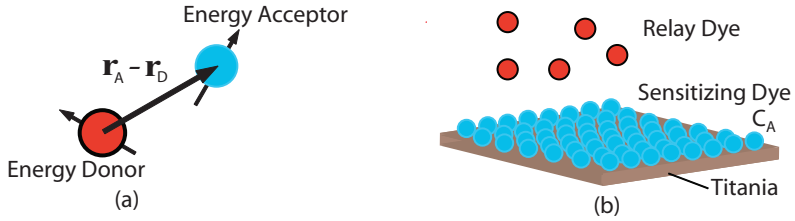

Fig. 1. (a) Geometries of FRET occurring from a single donor to a single acceptor and (b) from donors to a dense monolayer of acceptors with surface concentration C_A as in the case of a dye sensitized solar cell with relay dyes.

In our model, we assume that the energy donors are uniformly distributed inside a pore, and the energy acceptors are uniformly and densely distributed over the surface of the pore walls, described by a surface concentration C_A. If the average spacing between individual acceptor chromophores is small compared to the Förster radius ($C_A R_0^2 >> 1$), we can approximate the sum in Eq. (3) with an integral over the pore wall surface.

$$k_F\left(\mathbf{r_D}\right) = \frac{1}{\tau_0} \int_{S_A} \frac{C_A R_0^6}{\left|\mathbf{r_A} - \mathbf{r_D}\right|^6} \cdot dr_A^2 \tag{4}$$

DSC's typically have a C_A between 0.2 and 1 dye/nm^2 which is dependent upon the dye molecule size, number of attachment groups, the titania nanoparticle size, and whether or not a co-adsorbent is used that competes for the surface sites [19]. The errors associated with this approximation are most significant when the energy relay dye is a distance from the pore wall that is comparable or smaller than the spacing between the sensitizing dye molecules. In this case, the distance between a donor and the nearest acceptors is very small and thus the energy transfer rate is sensitive to the precise distances to these nearest acceptors. This is also the

#121278 - $15.00 USD Received 16 Dec 2009; revised 3 Feb 2010; accepted 6 Feb 2010; published 11 Feb 2010

regime where deviations from the Förster dipole approximation become significant and can be off by more than 50% for large chromophores [20]. Although these factors may have a significant impact on the rate of Förster transfer, they have a negligible effect on the excitation transfer efficiency since energy transfer is nearly 100% probable at this short donor-acceptor separation distance in a well designed system.

The presence of the redox couple in the electrolyte of dye sensitized solar cells can greatly increase the rate of non-radiative decay of the relay dye, providing a parasitic pathway for excitation decay that competes with energy transfer. Iodide and triiodide are perfect quenchers of many dye molecules meaning that a single collision with an excited dye results in quenching. This quenching can occur via electron transfer from iodide to the dye or the iodide can induce the excited dye to undergo intersystem crossing to its relatively non-emissive triplet state [21]. Dynamic quenching is described by the Stern-Volmer equation.

$$\frac{Q_{D,Q}}{Q_{D,0}} = \frac{\tau_Q}{\tau_0} = \left(1 + \tau_0 \sum\nolimits_j k_{q_j} \left[Q_j\right]\right)^{-1} \tag{5}$$

Here $[Q_j]$ is the concentration of quenching species j and k_{qj} is the bimolecular quenching coefficient for the dye-quencher combination, which is typically 10^9-10^{10} $M^{-1}s^{-1}$ for effective quenchers [17]. $Q_{D,0}$ and τ_0 are the photoluminescence quantum efficiency and lifetime of the donor in absence of the quenching species, while $Q_{D,Q}$ and τ_Q refer to these respective quantities when the quenching species are present. The degree of quenching is larger for relay dyes with a longer lifetime τ_0, assuming similar values for k_q, because it provides more time for the dye to collide with quenchers.

The Förster radius is the length scale over which Förster resonant energy transfer is efficient between a donor and a single acceptor. For a donor that can undergo energy transfer to a monolayer of acceptors of surface concentration C_A, or could be dynamically quenched by quenchers Q_j, we show that the length scale over which FRET is efficient is instead:

$$R_c = \left(\frac{C_A R_0^6}{1 + \tau_0 \sum\nolimits_j k_{q_j} \left[Q_j\right]}\right)^{1/4} \tag{6}$$

A large Förster radius between the relay and sensitizing dyes, a dense surface coverage of the sensitizing dye on the titania surface and a small degree of quenching of the relay dye by the electrolyte are all important in achieving a large critical energy transfer distance, R_c, and a high excitation transfer efficiency.

The ratio of the competing rates of energy transfer and quenching can be used to calculate the excitation transfer efficiency. The details of this calculation depend upon the extent that the relay dye diffuses, which can greatly increase the excitation transfer efficiency. Assuming that the diffusivity of dyes in a mesopore can be described by the Stokes-Einstein relation, a relay dye dissolved in acetonitrile with a hydrodynamic radius of 1 nm will have a diffusivity of around 0.6 nm^2/ns. Diffusion of the relay dye can be neglected when the relay dye diffusion length is small compared to the critical energy transfer distance, i.e. $\sqrt{6D\tau_Q} \ll R_c$. This is the case for relay dyes with short quenched fluorescence lifetimes of $\tau_Q \leq 1$ ns. In the so called rapid diffusion limit, the diffusion length is large compared to the average donor-acceptor separation distance [16], or roughly when $\sqrt{6D\tau_Q} \gg R_p$. where $2R_p$ is the diameter of the pore. For a typical pore diameter of $2R_p$ = 30 nm, which is produced by using standard 20 nm diameter titania particles emulsions, this limit is reached when $\tau_Q \geq 1$ μs. We also examine the regime for dyes with intermediate lifetimes to investigate the tradeoff in selecting dyes with longer lifetimes, which can diffuse farther but are more easily quenched.

#121278 - $15.00 USD Received 16 Dec 2009; revised 3 Feb 2010; accepted 6 Feb 2010; published 11 Feb 2010

3. Calculation results for pores of cylindrical and spherical geometry

3.1 Short lifetime relay dyes: excitation transfer efficiency in the absence of diffusion

Many organic dyes have a fluorescence lifetime between 0.5 and 10 ns [17]. Most are nearly perfectly quenched by iodide/triiodide resulting in an even shorter lifetime in the DSC electrolyte. Consequently diffusion can be ignored when using most organic dyes as a relay dye since the dye can only diffuse about a nanometer or less during its excited state lifetime, which typically has a negligible impact on the excitation transfer efficiency. The ETE from a stationary energy donor to a stationary group of acceptors is equal to the ratio of the rate the excited donor undergoes energy transfer to the total rate of all decay mechanisms of the excited donor:

$$\eta_{ETE}\left(\mathbf{r_D}\right)=\frac{k_F\left(\mathbf{r_D}\right)}{\tau_Q^{-1}+k_F\left(\mathbf{r_D}\right)} \tag{7}$$

The excitation transfer efficiency for an ensemble of static donors is equal to the average ETE of all of the donors [22]. If we assume that the donors are evenly distributed throughout the pore volume, we can calculate the overall excitation transfer efficiency for the pore by averaging Eq. (7) over all possible positions of the donor and using Eq. (4) and (5) for the rates of energy transfer and non-radiative decay.

$$\begin{aligned}\overline{\eta_{ETE}} &= \frac{1}{V}\int_V \eta_{ET}\left(\mathbf{r_D}\right)\cdot dr_D^3 = \frac{1}{V}\int_V 1-\left(1+\tau_Q k_f\left(\mathbf{r_D}\right)\right)^{-1}\cdot dr_D^3 \\ &= \frac{1}{V}\int_V 1-\left(1+\frac{\tau_Q}{\tau_0}\int_{S_A}\frac{C_A R_0^6}{\left|\mathbf{r_A}-\mathbf{r_D}\right|^6}\cdot dr_A^2\right)^{-1}\cdot dr_D^3 = \frac{1}{V}\int_V 1-\left(1+\int_{S_A}\frac{R_c^4\cdot dr_A^2}{\left|\mathbf{r_A}-\mathbf{r_D}\right|^6}\right)^{-1}\cdot dr_D^3\end{aligned} \tag{8}$$

Here V is the pore volume. In the limit of no donor chromophore diffusion, the excitation transfer efficiency only depends upon the geometrical shape of the pore, which sets the bounds of both integrals, and the critical energy transfer distance, R_c.

Equation (8) can be easily evaluated numerically for pores that are modeled as cylinders or spheres. We further approximate the cylindrical pores to have an infinite length, L, which is valid if the length of the pore is much deeper than the pore radius and the critical energy transfer distance. For both pore geometries, R is the radial distance from the donor to the center of the pore and R_p is the radius of the pore (Fig. 2(a) and (b)). The rate of FRET from a relay dye located a distance R from the center of the pore to sensitizing dyes on the pore walls can be calculated for both pore geometries by applying Eq. (4):

$$k_{F,cyl}\left(R\right)=\frac{1}{\tau_0}\int_{S_A}\frac{C_A R_0^6}{\left|\mathbf{r_A}-\mathbf{r_D}\right|^6}\cdot dr_A^2=\frac{1}{\tau_0}\int_{-\infty}^{\infty}\int_0^{2\pi}\frac{C_A R_0^6 R_p\, d\theta dz}{\left(\left(R_p\cos\left(\theta\right)-R\right)^2+\left(R_p\sin\left(\theta\right)\right)^2\right)} \tag{9}$$

$$k_{F,sph}\left(R\right)=\frac{1}{\tau_0}\int_0^{2\pi}\int_0^{\pi}\frac{C_A R_0^6 R_p^2\sin\left(\theta\right)d\theta d\phi}{\left(\left(R_p\cos\left(\theta\right)-R\right)^2+\left(R_p\sin\left(\theta\right)\right)^2\right)^3}=\frac{1}{\tau_0}\frac{C_A R_0^6}{R_p^4}\frac{4\pi\left(1+\frac{R^2}{R_p^2}\right)}{\left(1-\frac{R^2}{R_p^2}\right)^4} \tag{10}$$

For the limit of static donors, the excitation transfer efficiency for cylindrical and spherical pores can then be calculated from Eq. (8).

$$\overline{\eta_{ETE,cyl}}=\frac{1}{\pi R_p^2 L}\int_0^{R_p}\left(1-\left(1+\tau_Q k_{F,cyl}\left(R\right)\right)^{-1}\right)2\pi LR\,dR \tag{11}$$

#121278 - $15.00 USD Received 16 Dec 2009; revised 3 Feb 2010; accepted 6 Feb 2010; published 11 Feb 2010

$$\overline{\eta_{ETE,sph}} = \frac{3}{4\pi R_p^3}\int_0^{R_p}\left(1-\left(1+\tau_Q k_{F,sph}\right)^{-1}\right)4\pi R^2 dR = 1-3\int_0^1\left(1+64\pi\left(\frac{R_c}{2R_p}\right)^4\frac{1+r^2}{\left(1-r^2\right)^4}\right)^{-1} r^2 dr \quad (12)$$

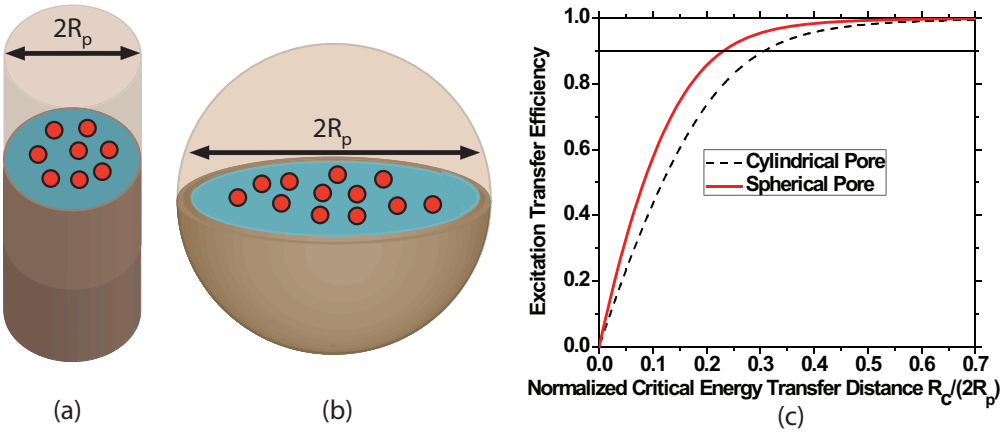

Fig. 2. (Color online) Geometries of the cylindrical (a) and spherical (b) pores of diameter $2R_p$. The relay dye is distributed throughout the volume of the interior of the pore while the sensitizing dye densely covers the pore walls. (c) Calculated excitation transfer efficiency in cylindrical (dotted curve) and spherical (solid curve) pores in the absence of diffusion as a function of the ratio of the critical energy transfer distance R_c to the pore diameter $2R_p$.

The excitation transfer efficiency only depends upon the ratio of the critical energy transfer distance to the diameter of the pore, which can be seen explicitly for the spherical case in Eq. (12). For an ETE of greater than 90% the critical energy transfer distance should be roughly a quarter to a third of the pore diameter or larger (Fig. 2(c)). For pore diameters of 30 nm, this corresponds to R_c > 9.2nm and R_c > 7.0nm respectively for cylindrical and spherical pores. For organic relay dyes in a DSC with a conventional iodide/triiodide electrolyte, quenching is nearly perfect with $k_q[Q]$ ~5x10^9 s^{-1} [3]. Assuming a sensitizing dye surface coverage of C_A = 0.5 dye molecules/nm^2, for a relay dye lifetime of τ_0 = 0.5ns, a minimum Förster radius of 6.07 nm or 5.03 nm is required to achieve 90% ETE for cylindrical and spherical pores respectively. If the (unquenched) lifetime of the dye were τ_0 = 5ns, however, only ~70% ETE would be achieved for these Förster radii due to increased quenching. There is thus considerable benefit of using shorter lifetime relay dyes to minimize the effects of quenching when nearly perfect quenching occurs.

In an actual mesoporous film, the pores are neither cylindrical nor spherical in shape. However, the difference in the calculated energy transfer efficiencies between these two geometries is not large so we would expect the ETE for actual pore geometries to be close to the results for the cylindrical and spherical pores. Mesoporous films have a distribution of pore sizes, which can be measured by the Brunauer, Emmett and Teller (BET) method. The theoretical average excitation transfer efficiency for the film can be determined by calculating the excitation transfer efficiency at each pore size and taking a weighted average of these values using the measured distribution of pore sizes.

3.2 Long lifetime relay dyes: excitation transfer efficiency in the rapid diffusion limit

Not all dyes are completely quenched by iodide and triiodide. For example, some lanthanide complexes can undergo thousands of collisions with iodide before being quenched and have bimolecular quenching coefficients of k_q < 10^6 M^{-1}s^{-1} [23]. For relay dyes that are relatively insensitive to collisional quenching, a long lifetime is highly beneficial for energy transfer since it enables the dye to diffuse closer to the pore wall, greatly reducing the critical energy transfer distance required for 90% excitation transfer efficiency. Eventually a longer diffusion

#121278 - $15.00 USD Received 16 Dec 2009; revised 3 Feb 2010; accepted 6 Feb 2010; published 11 Feb 2010

length leads to no further improvement in the ETE and this situation is referred to as the rapid diffusion limit. In this limit, a donor can move through nearly all of the different regions in the pore during its excited state lifetime ($\tau_Q \geq 1\mu s$ for 30 nm diameter pores). Consequently, all donors have the same average rate of undergoing energy transfer averaged over their excited state lifetime. This rate can be computed by averaging the energy transfer rate over all possible donor positions in the pore [16].

$$\overline{k_F} = \frac{1}{V_e}\int_{V_e} k_F\left(\mathbf{r_D}\right)\cdot dr_D^3 \tag{13}$$

Equation (13) diverges if the integration volume is taken as the full pore volume since this would allow the donor to diffuse arbitrarily close to acceptors on the pore wall where the rate of energy transfer approaches infinity in the Förster dipole model. The finite size of the donor and acceptor molecules needs to be considered when setting the bounds on the volume integration to set a minimum separation distance between the donors and acceptors. For small dye molecules, this distance of closest approach is around R_a = 0.5nm [16,17]. We use V_e to represent the volume in the pore that donors can occupy, which excludes the regions that are less than the distance of closest approach from the pore wall.

The average excitation transfer efficiency is equal to the ratio of the average rate of energy transfer to the average total decay rate [17] which combined with Eq. (4) and (6) yields:

$$\overline{\eta_{ETE}} = \frac{\overline{k_F}}{\tau_Q^{-1} + \overline{k_F}} = 1 - \left(1 + \frac{1}{V_e}\int_{V_e}\int_{S_A} \frac{R_c^4 \cdot dr_A^2}{\left|\mathbf{r_A} - \mathbf{r_D}\right|^6}\cdot dr_D^3\right)^{-1} \tag{14}$$

For the case of the cylindrical pore, the integrations need to be performed numerically. An analytic solution, however, exists for the sphere:

$$\overline{\eta_{ETE}} = 1 - \left(1 + \frac{3}{4\pi\left(R_p - R_b\right)^3}\int_0^{R_p - R_b} \tau_Q k_{F,sph} 4\pi R^2 dR\right)^{-1} = 1 - \left(1 + \left(\frac{R_c}{2R_p}\right)^4 \frac{\pi}{\left(1-b\right)^3 b^3}\right)^{-1} \tag{15}$$

Here R_a is the closest distance that the donor can be from the boundary of the pore and $b = R_a / (2R_p)$. The critical energy transfer distance required to achieve 90% ETE in a 30 nm diameter pore is shown in Fig. 3. The excitation transfer efficiency is higher for the spherical pores compared to the cylindrical pores for the same parameters, though the difference is again relatively small in the regime where the ETE is high. The excitation transfer efficiency is highly sensitive to the distance of closest approach, R_a, and consequently larger and bulkier relay and sensitizing dyes will have a lower ETE since they cannot get as close together. For a distance of closest approach of R_a = 0.5 nm, $R_c \geq 2$ nm is sufficient to get over 90% ETE for both pore geometries. If the impact of quenching is negligible, this critical energy transfer distance can be achieved with a Förster radius of only 1.8 nm, assuming C_A = 0.5 molecules/nm^2.

The challenge in selecting dyes to achieve high excitation transfer efficiencies in the rapid diffusion limit is finding dyes with sufficiently long lifetimes in the presence of the quenching DSC electrolyte to be in the rapid diffusion regime, roughly $\tau_Q \geq 1\mu s$. Many dyes, including metal-ligand complexes have lifetimes (τ_0) of a microsecond or more. However, from Eq. (5) the dye lifetime in the electrolyte is ultimately limited by the time scale over which quenching occurs: $\tau_Q < \left(\sum_j k_{q_j}\left[Q_j\right]\right)^{-1}$. The iodide concentration in the electrolyte needs to be at least 10^{20} ions/cm^3 [24,25], or 0.2 M, for efficient regeneration of the sensitizing dye to occur. Consequently relay dye molecules should be chosen with bimolecular quenching coefficients with iodide/triiodide of $k_q \leq 10^6$ M^{-1}s^{-1} in order to reach the rapid diffusion limit.

#121278 - $15.00 USD Received 16 Dec 2009; revised 3 Feb 2010; accepted 6 Feb 2010; published 11 Feb 2010

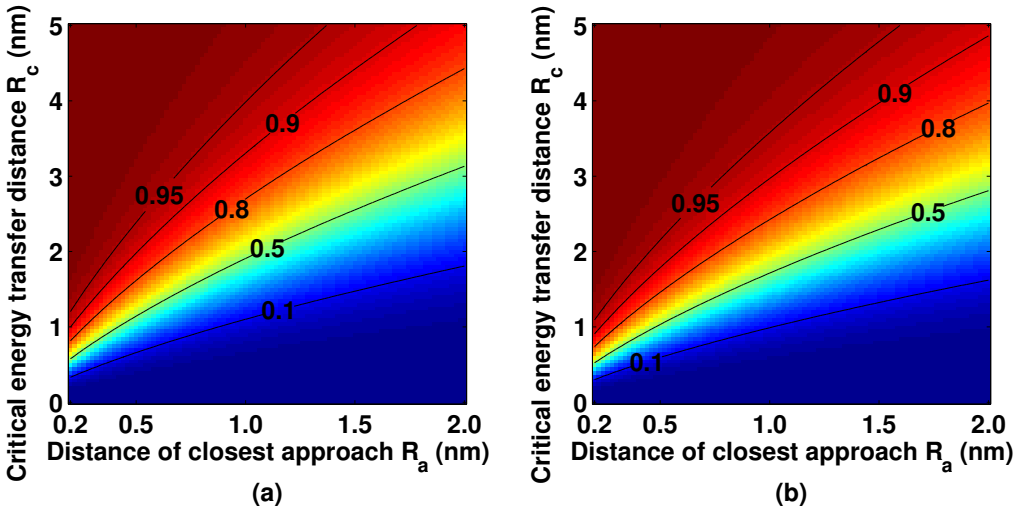

Fig. 3. (Color online) Excitation transfer efficiency in (a) cylindrical and (b) spherical pores in the rapid diffusion limit as a function of the critical energy transfer distance, R_c and the distance of closest approach that the donors can be from the pore wall, R_a. The pore diameter was assumed to be $2R_p$ = 30nm. To determine the excitation efficiency for other pore sizes, scale R_c and R_a by the same proportionality factor that R_p is changed.

Encapsulated structures, where the optically active region is surrounded by a protective shell, may be good relay dye candidates due to their reduced bimolecular quenching coefficients. Lanthanide cryptates have been demonstrated to have bimolecular quenching coefficients with iodide as low as $k_q = 10^2$ $M^{-1}s^{-1}$ [26]. Core-shell nanoparticles may be another possibility. The thickness of the protective shell should be as thin as possible without sacrificing its effectiveness, since the shell increases the distance of closest approach, R_a, reducing the excitation transfer efficiency.

3.3 Intermediate lifetime relay dyes: full model of the impact of relay dye lifetime on ETE

A longer relay dye lifetime allows the dye to diffuse further in the DSC electrolyte, improving the excitation transfer efficiency, but also increases the chances that it will be quenched, which lowers the ETE. To understand the effect of the relay dye lifetime on the ETE when diffusion and quenching are both significant, we need to examine the regime of intermediate diffusion. The general case for energy transfer in the presence of diffusion was treated by Steinberg et al. [15] who considered the survival probability distribution of the excited donor and derived a partial differential equation to describe the decay of this distribution. We summarize this method below, which we have adapted to include the effects of dynamic quenching.

At time $t = 0$, a single donor is excited somewhere inside the pore. $P(\mathbf{r_D}, t)$ is the survival probability, which is the probability density that the excited donor is at the position vector $\mathbf{r}$ after a delay of t following excitation. Since a random donor is excited, $P(t = 0)$ is equal to $1/V_e$ everywhere inside the pore where there could be a donor molecule and zero elsewhere. As in the case of the rapid diffusion limit, the donors are not permitted to be closer than the distance of closest approach, R_a, from the pore walls. The survival probability function evolves according to the following continuity equation, which accounts for diffusion, FRET and non-radiative decay of the donor:

$$\frac{\partial P(\mathbf{r_D}, t)}{\partial t} = \left(D\nabla^2 - k_f(\mathbf{r_D}) - \tau_Q^{-1} \right) P(\mathbf{r_D}, t) \qquad (16)$$

Here D is the diffusion coefficient of the donor species. We impose homogeneous Neumann boundary conditions, $\mathbf{n} \bullet \nabla P = 0$ (where $\mathbf{n}$ is the surface normal vector), to allow

#121278 - $15.00 USD Received 16 Dec 2009; revised 3 Feb 2010; accepted 6 Feb 2010; published 11 Feb 2010

for the possibility for donors to bounce off the pore wall without undergoing energy transfer, which can be significant if the donor's fluorescence lifetime is long or the minimum donor-acceptor separation distance is large, resulting in a slow FRET rate. The survival probability distribution can be in principle determined using a numerical partial differential equation solver to solve Eq. (16).

The excitation transfer efficiency is equal to the probability the excited donor does not undergo non-radiative decay. The integral of P over the pore volume gives us the probability that the donor has not yet decayed after time t, which approaches zero for times much longer than the lifetime of the donor. Multiplying this by the non-radiative decay rate and integrating over all time gives the probability that the excited donor undergoes non-radiative decay. Thus the excitation transfer efficiency is given by [27]:

$$\overline{\eta_{ETE}} = 1 - \int_0^\infty \tau_Q^{-1} \int_{V_e} P\left(\mathbf{r_D}, t\right) dr_D^3 dt \tag{17}$$

In the case of cylindrical and spherical pores, the survival distribution function P only depends upon the radial distance from the center of the pore, and Eq. (16) simplifies to:

$$\frac{\partial P\left(R,t\right)}{\partial t} = D \frac{1}{R^m} \frac{\partial}{\partial R}\left(R^m \frac{\partial P}{\partial R}\right) - \left(k_f\left(R\right) + \tau_Q^{-1}\right) P\left(R,t\right) \tag{18}$$

Here $m = 1$ in the case of the cylindrical pores and $m = 2$ for the spherical pores and k_f is given by Eq. (9) or (10). The initial condition to the problem is $P(t = 0) = 1/V_e$ inside the pore and zero outside, where V_e is the volume of a cylinder of radius $R_p - R_a$ and length L or of a sphere of radius $R_p - R_a$. We impose reflective boundaries at the pore walls and constrain the diffusion flux to be finite in the pore center:

$$\frac{\partial P\left(R = R_p - R_a, t\right)}{\partial t} = 0 \text{ and } \frac{\partial P\left(R = 0\right)}{\partial t} = 0 . \tag{19}$$

The partial differential equation can be solved numerically by discretizing P in space and time. The integrations in Eq. (17) can then be performed numerically to calculate the ETE. This method was checked in the static and rapid diffusion limits and was found to agree within 1% of the solutions found using the previously described models for those limits.

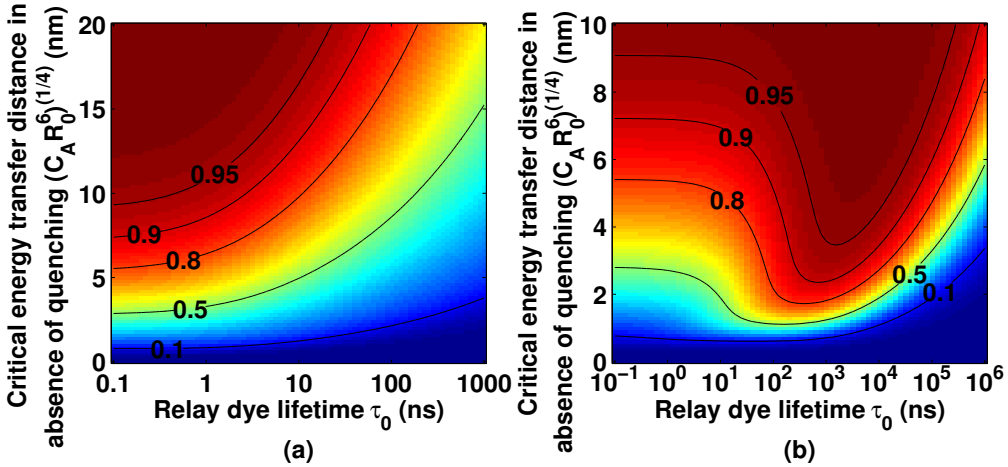

Fig. 4. (Color online) Excitation transfer efficiency for a spherical pore (a) with significant quenching ($k_q[Q] = 10^9 s^{-1}$) and (b) reduced quenching ($k_q[Q] = 10^6 s^{-1}$) as a function of the relay dye lifetime and critical energy transfer distance in absence of quenching. The pore diameter was set to $2R_p = 30$nm, the distance of closest approach was $R_a = 0.5$nm, and a relay dye diffusivity of $D = 0.6 nm^2/ns$ was used in these calculations.

#121278 - $15.00 USD Received 16 Dec 2009; revised 3 Feb 2010; accepted 6 Feb 2010; published 11 Feb 2010

The calculated excitation transfer efficiency for 30-nm-diameter spherical pores is shown above for the case when the relay dye is nearly perfectly quenched by the redox couple [Fig. 4(a), $k_q[Q] = 1\text{x}10^9\ s^{-1}$] and when the quenching is less severe [Fig. 4(b), $k_q[Q] = 1\text{x}10^6\ s^{-1}$]. In the case of nearly perfect quenching, the ETE decreases with relay dye lifetime because longer lived dyes allow more time to be quenched by the electrolyte. Diffusion plays a minor role since the dye lifetime in the electrolyte is limited to 1 ns and the dye will be quenched before it can diffuse appreciably. In the case of reduced quenching, longer lived dyes allow the relay dye to diffuse further, improving the ETE. The critical energy transfer distance required to achieve 90% ETE decreases by about a factor of three when the lifetime of the dye (τ_0) is increased from 1 ns to 1 μs, going from the static limit to the rapid diffusion limit. If the lifetime is increased further, however, the ETE begins to drop since quenching of the dye becomes significant. A longer dye lifetime is thus only beneficial when the lifetime is less than the time scale for quenching.

4. Discussion

The calculations for the cylindrical and spherical pores suggest two strategies for achieving excitation transfer efficiencies of over 90% in a dye sensitized solar cell with relay dyes. The first approach is to find relay and sensitizing dye combinations with moderately high Förster radii of 5 nm or more and relay dyes with short fluorescence lifetimes to minimize the chance that they will be quenched before they undergo energy transfer. A second strategy is to select a donor dye that is not easily quenched by triiodide ($k_q \leq 10^6\ M^{-1}s^{-1}$) and has a long lifetime of a microsecond or more. In this case the relay dye and sensitizing dye can have a small Förster radius of ~2 nm and still undergo efficient energy transfer due to diffusion. It may be easier adopting the first strategy and selecting relay dyes with short lifetimes since iodide quenching is so highly efficient for most dyes. We previously adopted this approach in selecting PTCDI as the relay dye which is highly fluorescent, ($Q_{D,0}$ = 90%) enabling a Forster radius of 7.5 nm with the sensitizing dye TT1, and has a short lifetime, (τ_0 = 4.8 ns) minimizing quenching [3]. For the second approach, ytterbium complexes appear to be the most promising for relay dyes of the lanthanide complexes as they emit at 980 nm [28] and would efficiently undergo energy transfer to a near infrared sensitizing dye.

In order to function in a DSC and harvest most of the incident photons, the relay and sensitizing dyes additionally must have strong and complementary absorption spectra [3]. The relay dye must either be highly soluble in the DSC electrolyte (typically acetonitrile) or have a high molar extinction coefficient. As an example, dyes with a peak molar extinction coefficient of 50,000 $M^{-1}\ cm^{-1}$ would need a concentration of ~40 mM to absorb 90% of the light in a 10 μm thick film; however dyes with twice the molar extinction coefficient (i.e. 100,000 $M^{-1}\ cm^{-1}$) would require half the concentration. The sensitizing dye should be able to pack densely on the titania surface and have good injection into the titania.

The model presented in this paper can be extended with some modifications to relay dyes in solid state dye sensitized solar cells. There is a great potential for energy relay dyes to improve the efficiency of solid state DSC's which are limited in thickness to 2 μm and cannot absorb all of the incident light. Recently we have demonstrated an improvement in the efficiency of a solid state DSC using a relay dye [29]. Unlike in the liquid electrolytic DSC, diffusion of the relay dye is not possible. Studies have suggested that the pores are not completely filled in solid state DSC and that there are voids of ~40% of the pore volume in the center of the pores [30]. Consequently, there is the potential for energy transfer to be more efficient in the solid state DSC since the relay dyes are not located in the center of the pore where energy transfer to the pore wall is the least efficient. Incomplete pore filling may make it difficult, however, to incorporate sufficient relay dye into the device to sufficiently absorb the higher energy photons.

#121278 - $15.00 USD Received 16 Dec 2009; revised 3 Feb 2010; accepted 6 Feb 2010; published 11 Feb 2010

5. Conclusion

Here we presented a model for calculating the excitation transfer efficiency from a general volume containing energy donors to a dense surface of acceptors, accounting for the processes of diffusion and quenching. For the application of dye sensitized solar cells with energy relay dyes, a large Förster radius between the relay and sensitizing dyes, a dense sensitizing dye surface concentration on the titania, relatively low bimolecular quenching coefficients between the relay dye and the redox couple, and small to moderate sized pores are all important for efficient excitation transfer. A large relay dye diffusivity and long fluorescence lifetime are also beneficial but only when quenching by the redox couple is insignificant. Otherwise a short lifetime is advantageous to avoid quenching. Using calculations for cylindrical and spherical pores we have demonstrated that the energy transfer process can be over 90% efficient in a dye sensitized solar cell with dyes with reasonable properties. Near unity excitation transfer efficiencies can be obtained using dyes combinations with a relatively large Förster radius where the donor has a short lifetime to avoid quenching effects or alternatively with a dye combination with a relatively small Förster radius, provided that the donor has a long fluorescence lifetime and is not significantly quenched by the electrolyte to enable diffusion.

Acknowledgements

This work was supported by the King Abdullah University of Science and Technology Center for Advanced Molecular Photovoltaics and the Office of Naval Research contract no. N00014-08-1-1163. E.T.H. was supported by the National Science Foundation GRFP and the Fannie and John Hertz Foundation.

#121278 - $15.00 USD Received 16 Dec 2009; revised 3 Feb 2010; accepted 6 Feb 2010; published 11 Feb 2010